

REPORT DOCUMENTATION PAGE			Form Approved OMB NO. 0704-0188		
<p>The public reporting burden for this collection of information is estimated to average 1 hour per response, including the time for reviewing instructions, searching existing data sources, gathering and maintaining the data needed, and completing and reviewing the collection of information. Send comments regarding this burden estimate or any other aspect of this collection of information, including suggestions for reducing this burden, to Washington Headquarters Services, Directorate for Information Operations and Reports, 1215 Jefferson Davis Highway, Suite 1204, Arlington VA, 22202-4302. Respondents should be aware that notwithstanding any other provision of law, no person shall be subject to any penalty for failing to comply with a collection of information if it does not display a currently valid OMB control number.</p> <p>PLEASE DO NOT RETURN YOUR FORM TO THE ABOVE ADDRESS.</p>					
1. REPORT DATE (DD-MM-YYYY) 02-05-2014		2. REPORT TYPE Final Report		3. DATES COVERED (From - To) 1-Oct-2009 - 31-Mar-2014	
4. TITLE AND SUBTITLE Multi-length Scale Material Model Development for Armor-grade Composites			5a. CONTRACT NUMBER W911NF-09-1-0513		
			5b. GRANT NUMBER		
			5c. PROGRAM ELEMENT NUMBER 622105		
6. AUTHORS Mica Grujicic			5d. PROJECT NUMBER		
			5e. TASK NUMBER		
			5f. WORK UNIT NUMBER		
7. PERFORMING ORGANIZATION NAMES AND ADDRESSES Clemson University 300 Brackett Hall Box 345702 Clemson, SC 29634 -5702			8. PERFORMING ORGANIZATION REPORT NUMBER		
9. SPONSORING/MONITORING AGENCY NAME(S) AND ADDRESS (ES) U.S. Army Research Office P.O. Box 12211 Research Triangle Park, NC 27709-2211			10. SPONSOR/MONITOR'S ACRONYM(S) ARO		
			11. SPONSOR/MONITOR'S REPORT NUMBER(S) 56526-EG.19		
12. DISTRIBUTION AVAILABILITY STATEMENT Approved for Public Release; Distribution Unlimited					
13. SUPPLEMENTARY NOTES The views, opinions and/or findings contained in this report are those of the author(s) and should not be construed as an official Department of the Army position, policy or decision, unless so designated by other documentation.					
14. ABSTRACT The present work was focused on establishing microstructure/property relationships in p-phenylene terephthalamide (PPTA) based materials and structures. A multi-length-scale computational approach has been developed in order to identify and quantify the contribution of various microstructural features and processes, at different length-scales, to the macroscopic-level ballistic-penetration resistance of PPTA-based fabric or PPTA-fiber-reinforced polymer-matrix composites. Specifically, the role of various material-synthesis-/fiber-processing-induced defects, as well as defects induced during the weaving process, was investigated. The results obtained clearly revealed that					
15. SUBJECT TERMS Armor-grade Composites; Multi-length Scale Material Model Development					
16. SECURITY CLASSIFICATION OF:			17. LIMITATION OF ABSTRACT UU	15. NUMBER OF PAGES	19a. NAME OF RESPONSIBLE PERSON Mica Grujicic
a. REPORT UU	b. ABSTRACT UU	c. THIS PAGE UU			19b. TELEPHONE NUMBER 864-656-5639

Report Title

Multi-length Scale Material Model Development for Armor-grade Composites

ABSTRACT

The present work was focused on establishing microstructure/property relationships in p-phenylene terephthalamide (PPTA) based materials and structures. A multi-length-scale computational approach has been developed in order to identify and quantify the contribution of various microstructural features and processes, at different length-scales, to the macroscopic-level ballistic-penetration resistance of PPTA-based fabric or PPTA-fiber-reinforced polymer-matrix composites. Specifically, the role of various material-synthesis-/fiber-processing-induced defects, as well as defects induced during the weaving process, was investigated. The results obtained clearly revealed that both the static mechanical material properties such as stiffness and strength, and the dynamic-impact properties such as V50, are affected by the type and the concentration of various defects. Lastly, it was demonstrated that in order to construct a high-fidelity continuum-level PPTA-based material constitutive model, the role of the material microstructure (including defects) at different length-scales must be taken into account.

Enter List of papers submitted or published that acknowledge ARO support from the start of the project to the date of this printing. List the papers, including journal references, in the following categories:

(a) Papers published in peer-reviewed journals (N/A for none)

<u>Received</u>	<u>Paper</u>
04/09/2014 17.00	M. Grujicic, B. Pandurangan, J. S. Snipes, C.-F. Yen, B. A. Cheeseman. Multi-Length Scale-Enriched Continuum-Level Material Model for Kevlar®-Fiber-Reinforced Polymer-Matrix Composites, Journal of Materials Engineering and Performance, (03 2013): 681. doi: 10.1007/s11665-012-0329-6
04/09/2014 16.00	Mica Grujicic, Subrahmanian Ramaswami, Jennifer Snipes, Ramin Yavari, Gary Lickfield, Chian-Fong Yen, Bryan Cheeseman. Molecular-level computational investigation of mechanical transverse behavior of p-phenylene terephthalamide (PPTA) fibers, Multidiscipline Modeling in Materials and Structures, (09 2013): 462. doi: 10.1108/MMMS-11-2012-0018
04/27/2012 2.00	M. Grujicic, W. C. Bell, T. He, G. Arakere, B. A. Cheeseman, K. L. Koudela, J. F. Tarter. A COMPUTATIONAL INVESTIGATION OF IMPACT INTO MULTI-PLIES OF PLAIN-WOVEN FABRIC, Proceedings of the 2008 Fall SAMPE Technical Conference, (09 2008): 1. doi:
04/27/2012 13.00	M. Grujicic, A. Hariharan, B. Pandurangan, C.-F. Yen, B. A. Cheeseman, Y. Wang, Y. Miao, J. Q. Zheng. Fiber-Level Modeling of Dynamic Strength of Kevlar® KM2 Ballistic Fabric, Journal of Materials Engineering and Performance, (07 2011): 0. doi: 10.1007/s11665-011-0006-1
04/27/2012 12.00	M. Grujicic, B. Pandurangan, B. A. Cheeseman, C.-F. Yen. Spall-Fracture Physics and Spallation-Resistance-Based Material Selection, Journal of Materials Engineering and Performance, (10 2011): 0. doi: 10.1007/s11665-011-0068-0
04/27/2012 10.00	M. Grujicic, B. Pandurangan, W.C. Bell, C.-F. Yen, B.A. Cheeseman. Application of a dynamic-mixture shock-wave model to the metal-matrix composite materials, Materials Science and Engineering: A, (10 2011): 8187. doi: 10.1016/j.msea.2011.08.008
04/27/2012 9.00	M. Grujicic, P. S. Glomski, B. Pandurangan, W. C. Bell, C-F. Yen, B. A. Cheeseman. Multi-length scale computational derivation of Kevlar® yarn-level material model, Journal of Materials Science, (02 2011): 4787. doi: 10.1007/s10853-011-5389-8
04/27/2012 8.00	M. Grujicic, W. C. Bell, P. S. Glomski, B. Pandurangan, C.-F. Yen, B. A. Cheeseman. Filament-Level Modeling of Aramid-Based High-Performance Structural Materials, Journal of Materials Engineering and Performance, (11 2011): 1401. doi: 10.1007/s11665-010-9786-y
04/27/2012 7.00	M. Grujicic, T. He, H. Marvi, B. A. Cheeseman, C. F. Yen. A comparative investigation of the use of laminate-level meso-scale and fracture-mechanics-enriched meso-scale composite-material models in ballistic-resistance analyses, Journal of Materials Science, (06 2010): 3136. doi: 10.1007/s10853-010-4290-1
04/27/2012 6.00	Mica Grujicic, Bhaskar Pandurangan, Tao He, Guruprasad Arakere, William C. Bell, Patrick S. Glomski, Bryan A. Cheeseman. Material Modeling and Dynamic-Response Analysis of Resin-starved Cross-collimated Compliant Composites, Proceedings of the 1st Joint Canadian & American Technical Conference, (09 2009): 1. doi:
04/27/2012 5.00	M. Grujicic, W. C. Bell, G. Arakere, T. He, X. Xie, B. A. Cheeseman. Development of a Meso-Scale Material Model for Ballistic Fabric and Its Use in Flexible-Armor Protection Systems, Journal of Materials Engineering and Performance, (02 2010): 22. doi: 10.1007/s11665-009-9419-5
04/27/2012 4.00	M. Grujicic, P. S. Glomski, T. He, G. Arakere, W. C. Bell, B. A. Cheeseman. Material Modeling and Ballistic-Resistance Analysis of Armor-Grade Composites Reinforced with High-Performance Fibers, Journal of Materials Engineering and Performance, (02 2009): 1169. doi: 10.1007/s11665-009-9370-5

04/27/2012	3.00	M. Grujicic, G. Arakere, T. He, W.C. Bell, P.S. Glomski, B.A. Cheeseman. Multi-scale ballistic material modeling of cross-ply compliant composites, Composites Part B: Engineering, (09 2009): 468. doi: 10.1016/j.compositesb.2009.02.002
04/27/2012	1.00	M. Grujicic, G. Arakere, T. He, W.C. Bell, B.A. Cheeseman, C.-F. Yen, B. Scott. A ballistic material model for cross-ply unidirectional ultra-high molecular-weight polyethylene fiber-reinforced armor-grade composites, Materials Science and Engineering: A, (12 2008): 231. doi: 10.1016/j.msea.2008.07.056
10/21/2013	15.00	M. Grujicic, S. Ramaswami, J. S. Snipes, R. Yavari, C.-F. Yen, B. A. Cheeseman. Axial-Compressive Behavior, Including Kink-Band Formation and Propagation, of Single p-Phenylene Terephthalamide (PPTA) Fibers, Advances in Materials Science and Engineering, (08 2013): 0. doi: 10.1155/2013/329549
10/21/2013	14.00	M. Grujicic, R. Yavari, S. Ramaswami, J. S. Snipes, C.-F. Yen, B. A. Cheeseman. Molecular-Level Study of the Effect of Prior Axial Compression/Torsion on the Axial-Tensile Strength of PPTA Fibers, Journal of Materials Engineering and Performance, (07 2013): 0. doi: 10.1007/s11665-013-0648-2

TOTAL: 16

Number of Papers published in peer-reviewed journals:

(b) Papers published in non-peer-reviewed journals (N/A for none)

<u>Received</u>	<u>Paper</u>
04/27/2012	11.00 M. Grujicic, W.C. Bell, B. Pandurangan, C.-F. Yen, B.A. Cheeseman. Computational investigation of structured shocks in Al/SiC-particulate metal-matrix composites, Multidiscipline Modeling in Materials and Structures, (06 2011): 469. doi:

TOTAL: 1

Number of Papers published in non peer-reviewed journals:

(c) Presentations

Non Peer-Reviewed Conference Proceeding publications (other than abstracts):

Received Paper

TOTAL:

Number of Non Peer-Reviewed Conference Proceeding publications (other than abstracts):

Peer-Reviewed Conference Proceeding publications (other than abstracts):

Received Paper

TOTAL:

Number of Peer-Reviewed Conference Proceeding publications (other than abstracts):

(d) Manuscripts

Received Paper

04/09/2014 18.00 M. Grujicic , J. S. Snipes , S. Ramaswami , R. Yavari, C.-F. Yen , B. A. Cheeseman. Analysis of Steel-with-Composite Material Substitution in Military-Vehicle Hull-Floors Subjected to Shallow-Buried Landmine-Detonation Loads, Multidiscipline Modeling in Materials and Structures (01 2014)

TOTAL: 1

Number of Manuscripts:

Books	
Received	Paper

TOTAL:

Patents Submitted

Patents Awarded

Awards

1. Eastman Chemical Faculty Excellence Award, 2012.
2. 2012 SAGE Best Paper Award
M Grujicic, W. C. Bell, B. Pandurangan, B. A. Cheeseman, C. Fountzoulas, P. Patel, D. W. Templeton, and K. D. Bishnoi, “The effect of high-pressure densification on ballistic-penetration resistance of a soda-lime glass”, Journal of Materials: Design and Applications, 225(4), pp. 298-315, 2011.
3. Emerald Publishing Literati Network Awards for Excellence 2011
M. Grujicic, H. Marvi, G. Arakere, W. C. Bell, I. Haque, “The Effect of Up-armoring the High-Mobility Multi-purpose Wheeled Vehicle (HMMWV) on the Off-road Vehicle Performance,” Multidiscipline Modeling in Materials and Structures, 6(2), 2010, 229-256.
4. Alumni Award for Outstanding Achievement in Research, April 2011
5. 2009 PE Publishing Prize
M. Grujicic, T. He, B. Pandurangan, W. C. Bell, N. Coutris, B. A. Cheeseman, W. N.Roy and R. R. Skaggs, “Development, Parameterization and Validation of a Visco-Plastic Material Model for Sand With Different Levels of Water Saturation”, Journal of Materials: Design and Applications, 223, pp. 63-81, 2009

Graduate Students

NAME	PERCENT SUPPORTED	Discipline
Guruprasad Arakere	0.14	
W. Cameron Bell	0.14	
Patrick Glomski	0.14	
Ajay Prasad Arakere	0.14	
Ramin Yavari	0.14	
Rohan Galgalikar	0.14	
Varun Chenna	0.14	
FTE Equivalent:	0.98	
Total Number:	7	

Names of Post Doctorates

<u>NAME</u>	<u>PERCENT SUPPORTED</u>
Bhaskar Pandurangan	0.25
Brian d'Entremont	0.25
Jennifer Snipes	0.25
Subrahmanian Ramaswami	0.25
FTE Equivalent:	1.00
Total Number:	4

Names of Faculty Supported

<u>NAME</u>	<u>PERCENT SUPPORTED</u>	National Academy Member
Mica Grujicic	0.10	No
FTE Equivalent:	0.10	
Total Number:	1	

Names of Under Graduate students supported

<u>NAME</u>	<u>PERCENT SUPPORTED</u>
FTE Equivalent:	
Total Number:	

Student Metrics

This section only applies to graduating undergraduates supported by this agreement in this reporting period

The number of undergraduates funded by this agreement who graduated during this period: 0.00

The number of undergraduates funded by this agreement who graduated during this period with a degree in science, mathematics, engineering, or technology fields:..... 0.00

The number of undergraduates funded by your agreement who graduated during this period and will continue to pursue a graduate or Ph.D. degree in science, mathematics, engineering, or technology fields:..... 0.00

Number of graduating undergraduates who achieved a 3.5 GPA to 4.0 (4.0 max scale):..... 0.00

Number of graduating undergraduates funded by a DoD funded Center of Excellence grant for Education, Research and Engineering:..... 0.00

The number of undergraduates funded by your agreement who graduated during this period and intend to work for the Department of Defense 0.00

The number of undergraduates funded by your agreement who graduated during this period and will receive scholarships or fellowships for further studies in science, mathematics, engineering or technology fields: 0.00

Names of Personnel receiving masters degrees

<u>NAME</u>	
Patrick Glomski	
Ajay Prasad Arakere	
Ramin Yavari	
Total Number:	3

Names of personnel receiving PHDs

<u>NAME</u>	
Guru Prasad Arakere	
W. Cameron Bell	
Total Number:	2

Names of other research staff

NAME

PERCENT SUPPORTED

FTE Equivalent:

Total Number:

Sub Contractors (DD882)

Inventions (DD882)

Scientific Progress

See attachment.

Technology Transfer

Project Title:
“Multi-length Scale Material Model Development for Armor-grade Composites”

ARO Proposal Number: 56526-EG

ARO Grant Number: W911-NF-09-1-0513

Project Period: 10/01/2009 to 03/31/2014

Mica Grujicic (PI)

Department of Mechanical Engineering, Clemson University

241 Fluor Daniel EIB, Clemson University, Clemson, SC 29634-0921

Table of Contents

1. Subject Materials	2
2. Problem Statement and Objective	2
3. Approach	3
4. Relevance to the Army	3
5. Accomplishments	3
6. Bibliography	22

1. Subject Materials

The work carried out under the present grant involves high specific-strength, high specific-stiffness p-phenylene terephthalamide (PPTA) polymeric fiber/filament (e.g. Kevlar[®], Twaron[®], etc.) based materials and structures. These materials/structures are commonly used in various protective systems whose main requirement is a high level of penetration resistance against high-kinetic-energy projectiles (e.g. bullets, mine, IED or turbine fragments, etc.). Their high mass-efficiency (i.e. mass-normalized performance) makes these materials and structures particularly suitable for use in applications such as protective garments for personnel extremity protection, interior spall liners in infantry vehicles, and a lining/shroud for turbine-fragment containment. The polymeric fibers/filaments are normally used as either thread constituents in two-dimensional or three-dimensional woven-fabric structures or as reinforcements in high-performance (typically) polymer-matrix composites.

2. Problem Statement and Objectives

Development of the aforementioned protection systems is traditionally carried out using legacy knowledge and extensive fabricate-and-test procedures. Since this approach is not only economically unattractive, but is often associated with significantly longer lead times, it has gradually become complemented by the appropriate cost- and time-efficient Computer Aided Engineering (CAE) analyses. This trend has been accelerated by the recent developments in the numerical modeling of transient non-linear dynamics phenomena such as those accompanying blast and ballistic loading conditions. However, the tools used in these analyses themselves suffer from a number of deficiencies/limitations which prevent these analyses from being more widely utilized. In the context of the use of CAE analyses for development of the aforementioned protection systems, it is well established that one of the main deficiencies stems from the inability of currently available material models to realistically represent the response of these materials under high-deformation rate, large-strain, high-pressure loading conditions, the conditions typically encountered during projectile impact events. One of the reasons for the indicated short comings of the present material models is a lack of inclusion of the contribution of various phenomena and processes occurring at different length scales to the overall behavior/performance of the

material. The main objective of the present work was to identify and quantify the contributions of the key molecule-/fibril-/fiber-/yarn-/ply-scale microstructural features (including the defect structure) to the mechanical performance of the materials at hand.

3. Approach

To address the problem described in the previous section, a multi-length-scale computational approach combining: (a) quantum-mechanical calculations; (b) all-atom molecular-level techniques; (c) coarse-grained meso-scale analyses; (d) discrete-element methods; and (e) continuum-level approaches are utilized. The computational methods and tools utilized at different length-scales are combined into a multi-scale computational framework, which enables interactions and linking of (i.e. data-exchange between) different analyses.

4. Relevance to the Army

In order to respond to the new enemy threats and warfare tactics, military systems, in particular those supporting the U.S. ground forces, are being continuously transformed to become faster, more agile, and more mobile so that they can be quickly transported to operations conducted throughout the world. Consequently, an increased emphasis is being placed on the development of improved lightweight body-armor and lightweight vehicle-armor systems as well as on the development of new high-performance armor materials. High-performance fiber-based materials, such as PPTA-based materials, have been exploited for both body-armor (e.g. as soft, flexible fiber mats for personal-armor vests) and for the vehicle-armor systems (e.g. as reinforcements in rigid polymer matrix composites, PMCs, for lightweight vehicle-armor systems). Establishment of the basic functional relationships between the material microstructure (at different length-scales and the material's ballistic-impact resistance, the subject of the present work, is critical as the Army is trying to develop a new generation of lightweight protective materials.

5. Accomplishments

Significant progress/accomplishments have been achieved in the following aspects of the project: (a) identification of the key microstructural length-scales in PPTA-based materials; (b) identification of the key synthesis-/processing-induced defects; (c) effect of

synthesis-/processing-induced defects on PPTA-fiber properties; (d) effect of fiber-/yarn-handling-induced defects on PPTA-fiber properties; (e) development of a continuum-level physically-based material constitutive model.

5.1 Identification of the Key Microstructural Length-Scales in PPTA-Based Materials

In our work reported in Refs. [1, 2], the hierarchical nature of the PPTA-based materials was investigated. This work identified eight microstructural length-scales, schematics and explanations of which are provided in Figure 1. The first column in this figure shows a set of simple schematics of the material microstructure/architecture at a given length-scale along with the labels used to denote the main microstructural constituents. In the second column, a brief description is provided of the material models used to capture the material behavior at the length-scale in question. A brief description of the material microstructure/ architecture and the corresponding material models at each of the length-scales listed in Figure 1 is provided below:

Laminate length-scale: At this length-scale, the material possesses no discernable microstructural features, i.e. it is completely homogenized. An example of the laminate-length scale composite material model can be found in Ref. [3].

Stacked-lamina length-scale: At this length-scale, the presence of discrete stacked laminae is recognized while the material within each lamina as well as inter-lamina boundaries are kept featureless/homogenized. An example of the composite material model at this length-scale can be found in Ref. [4].

Single-lamina length-scale: In this case, the microstructure/architecture of the reinforcement and matrix phases are explicitly taken into account while the two associated materials are treated as featureless/homogenized. The resulting “two-phase” composite-lamina model for each lamina is then combined with a fully-homogenized lamina/lamina interface model to form a stacked-lamina composite laminate structure. An example of this type of material model can be found in Ref. [5].

Fabric Unit-cell length-scale: At this length-scale, a closer look is given to the architecture of the woven fabric. Specifically, details of yarn weaving and crimping, yarn cross-section change, and yarn sliding at the warp-yarn/weft-yarn cross-over points are taken into account.

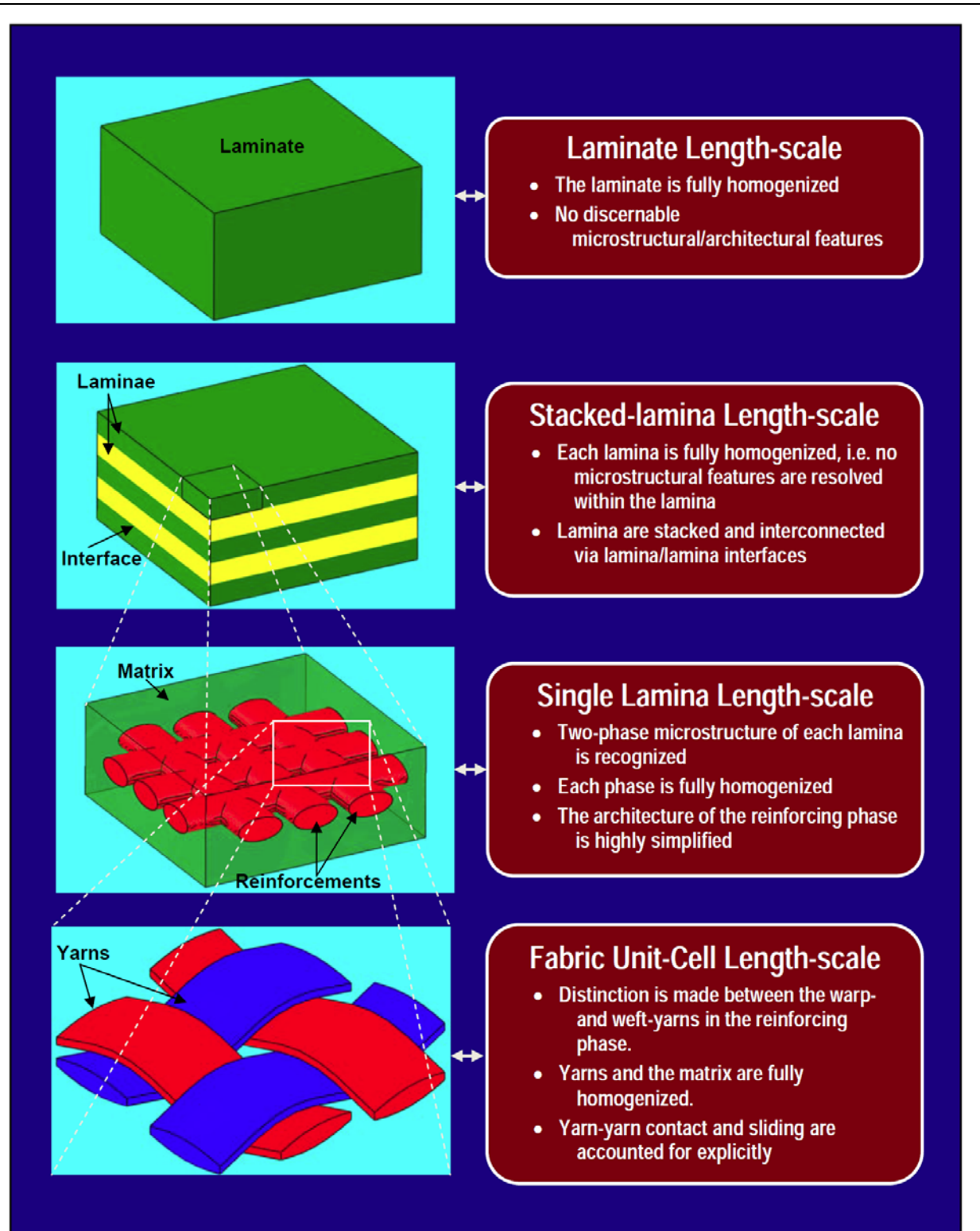


Figure 1. Various length-scales and the associated material model assumptions/simplifications used in the study of polymer-matrix composite materials with high-performance fiber-based structures.

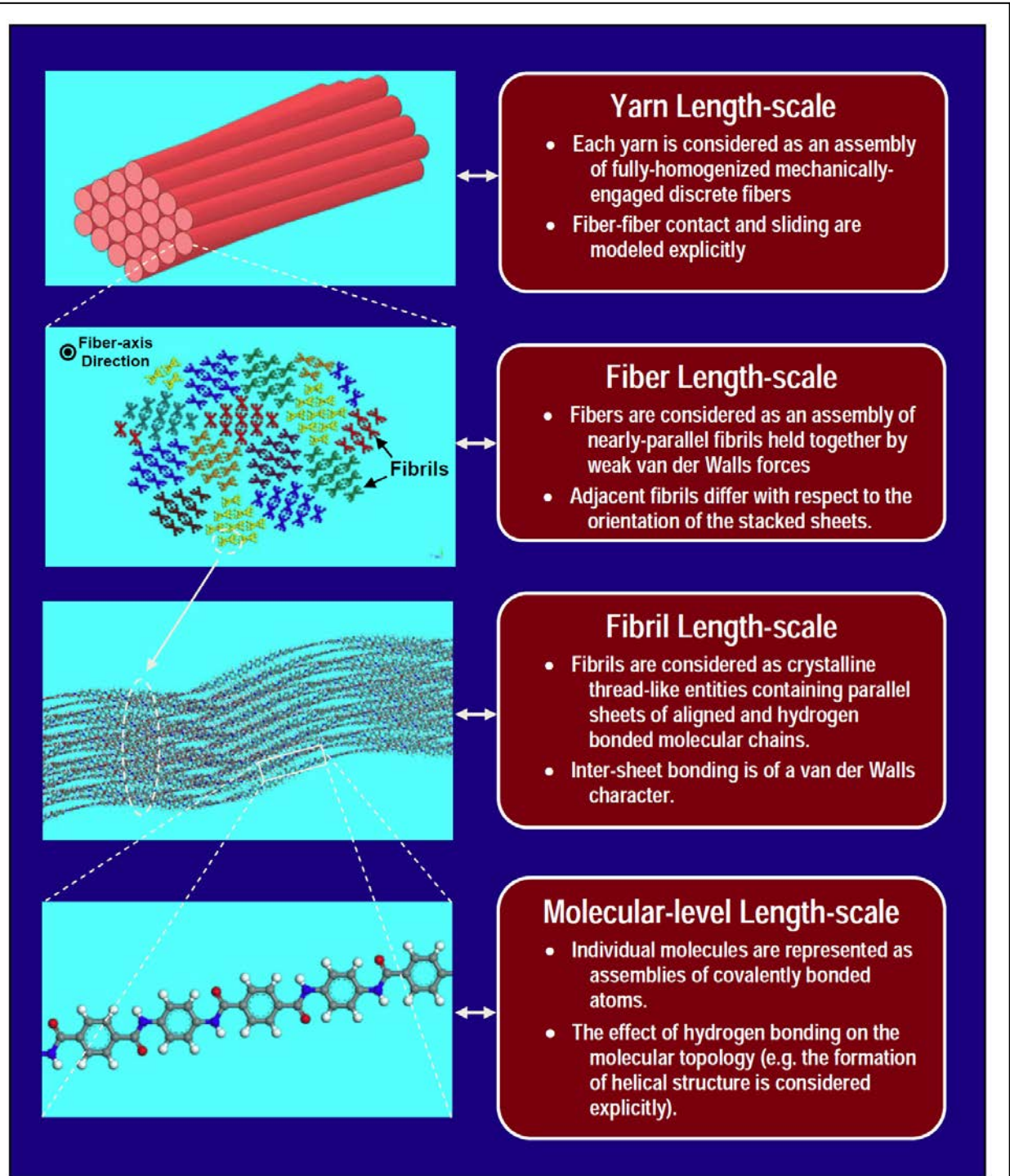


Figure 1. continued.

Each yarn is fully homogenized in this case as are the matrix and the lamina/lamina interfaces. An example of the model of this type can be found in Refs. [6-8].

Yarn length-scale: In this case, the internal structure/architecture of each yarn is accounted for explicitly. In other words, yarns are considered as assemblies of nearly parallel fibers/filaments which are mechanically engaged by either the application of a light twist to the yarn or by wrapping a fiber around the fiber/filament assembly. Typically, the detailed microstructure of the yarns is not incorporated into material models used in large-scale simulations of projectile/protection-system impact interactions (due to the unmanageably large computer resources needed). Instead, computational results of the mechanical response of the individual yarns, when subjected to a variety of loading conditions, are used to enrich the homogenized material model for the yarns. The latter is subsequently used at the fabric unit-cell length scale. An example of this approach can be found in Ref. [9].

Fiber length-scale: At this length-scale, fibers are considered as assemblies of aligned long-chain molecules which are held together by non-bond (van der Waals or Coulomb) forces. In the case of Kevlar[®] type fibers, there is a substantial experimental support for the existence of fibrils within the fibers. Fibrils are smaller bundles of molecular chains within which chain molecules are tightly bonded into a perfect or nearly perfect crystalline phase. Thus, in the case of Kevlar[®] type fibers, fibers can be considered as an assembly of fibrils. At this length-scale, the material is modeled using an all-atom/molecular approach within which the constituent discrete particles (atoms or ions) interact via valence-bond and non-bond forces. As in the previous case, the knowledge gained at the fiber length-scale is used to enrich the material description at the next level length-scale (the yarn length-scale, in the present case) and is not directly used in the large-scale modeling of projectile/protective-structure interactions.

Fibril-level length-scale: As mentioned above, within the fibrils the molecular structure is crystalline or nearly crystalline. However, the material at this length-scale (as well as the fiber length-scale) may contain a variety of material-synthesis-/fiber-manufacturing-induced microstructural and topological defects and chemical impurities which may significantly alter its properties. As in the fiber length-scale case, the material is treated as a collection of

discrete interacting/bonded particles and analyzed using the aforementioned atomic/molecular modeling tools/procedures.

Molecular chain-level length-scale: At this length-scale, chemical structure and conformation of the individual molecules constituting the chain is analyzed using the aforementioned atomic-/molecular-modeling tools/procedures. The main goal of the analysis at this length-scale is to identify the most-likely molecular conformations present in the molecules and, thus, fibrils. This greatly reduces the computational cost expended at the fibril and fiber length-scales.

5.2 Identification of the Key Synthesis-/Processing-Induced Defects

As in most engineering materials, properties of PPTA fibers are greatly affected by the presence of various defects/flaws. These flaws can be introduced during PPTA synthesis and PPTA-fiber fabrication processes. In the present work, the key steps associated with PPTA synthesis and PPTA-fiber processing have been analyzed in detail. This analysis identified the main synthesis-/processing-induced defects in PPTA fibers. A summary of the PPTA fiber most common defects, their dimensionality, their cause, ways of reducing their density, and their typical concentrations is provided in Table 1. These defects are expected to have a profound effect on the fiber properties, as well as on the properties of coarser-scale materials and structures containing PPTA fibers (e.g. yarns, fabric-ply, lamina and laminates).

5.3. Effect of Synthesis-/Processing-Induced Defects on PPTA-Fiber Properties

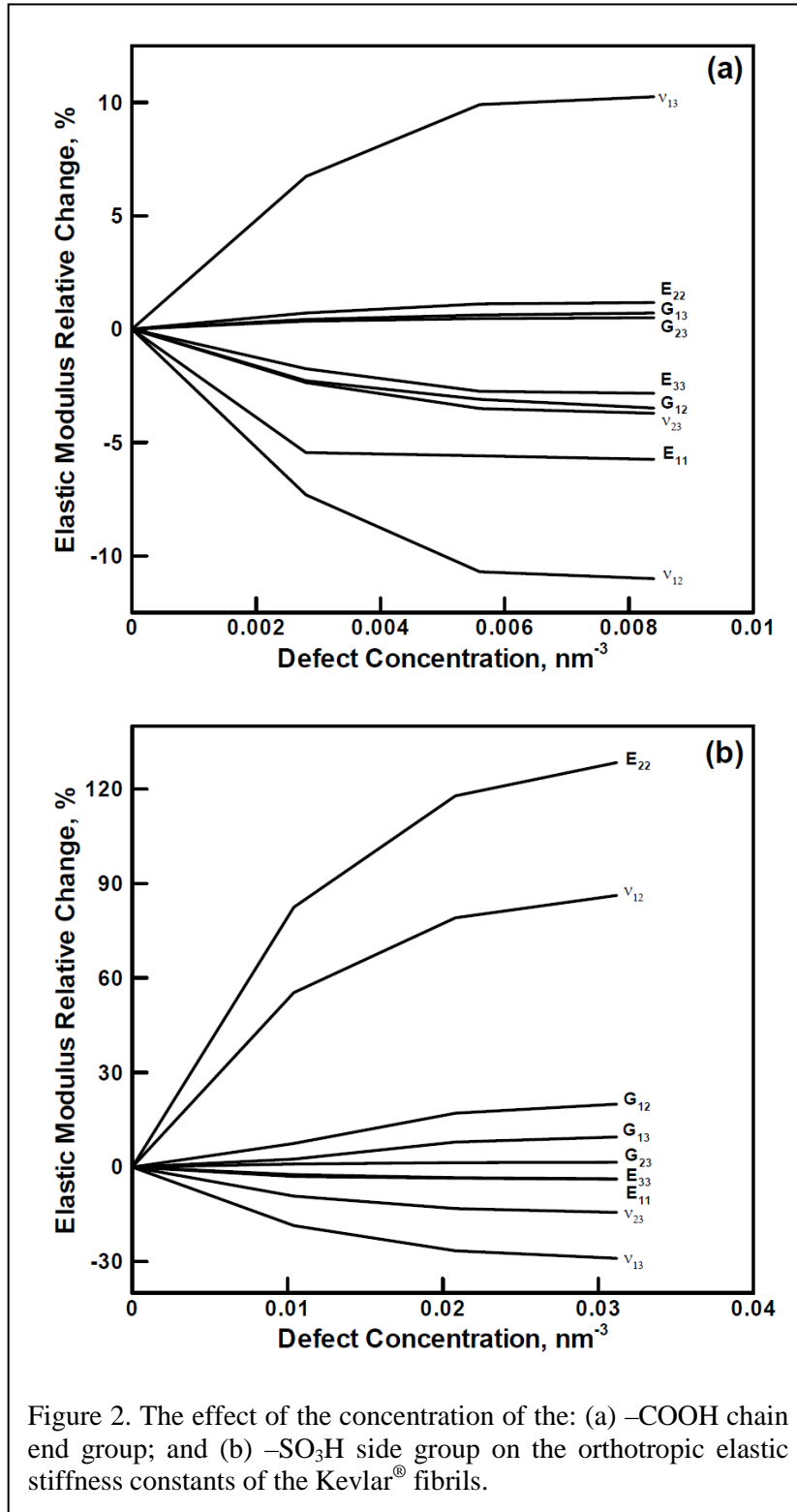
In this section, a brief summary is provided of the main results obtained in the present work, in which all-atom molecular-level modeling was used to establish the effect of various defects on the material properties (primarily strength and stiffness). This involved the use of a procedure to establish relationships between topology/kinematics and properties of PPTA fibrils, fibers and yarns, Figures 1(e)–(g).

Within the analysis carried out in the present work, it was demonstrated that the longitudinal stiffness, strength and ductility of the fibrils make the dominant contribution to the corresponding fiber and, in turn, yarn properties. As far as the transverse strength of fibers and yarns are concerned, they are found to be controlled by weak inter-fibril (and in

Table 1. A summary of most common defects found in Kevlar®-based materials

Flaw Group	Flaw	Causes	How causes can be remedied/mitigated	Range for concentration
Isolated chain ends (point defect)	-COOH	H ₂ SO ₄ catalyzed hydrolysis causing PPTA chain scission. Na ⁺ deficiency with respect to complete neutralization of side/end acidic groups.	Use concentrated H ₂ SO ₄ for dope preparation. Shorten the fiber wash time	0.35 per PPTA chain for each flaw* (~350 ppm-mass-based)
	-NH ₂	H ₂ SO ₄ catalyzed hydrolysis causing PPTA chain scission. Na ⁺ deficiency with respect to complete neutralization of side/end acidic groups.	Use higher concentration NaOH solution	0.35 per PPTA chain for each flaw* (~350 ppm-mass-based)
	-COO ⁻ Na ⁺	COOH neutralization with Na ⁺	No remedy required since this is one of the preferred chain ends	1.1 per PPTA chain* (~1100 ppm-mass-based)
	-NH ₃ ⁺ HSO ₄ ⁻	Sulfonation of the NH ₂ chain ends	Increase the H ₂ SO ₄ removal and neutralization rate	0.2 per PPTA chain* (~200 ppm-mass-based)
Side Groups (point defect)	-SO ₃ H	Exposure of PPTA in the dope to concentrated H ₂ SO ₄ (sulfonation)	Reduce the H ₂ SO ₄ concentration in the dope	~1300 ppm (mass-based)
	-SO ₃ ⁻ Na ⁺	Neutralization of sulfonic acid side groups by NaOH	Remedy may not be required since this side group improves fiber longevity. However mechanical performance may be compromised	~2500 ppm (mass-based)
Voids and Interstitials (point defects)	Microvoids	Swelling induced by hydration of intra-fibrillar Na ₂ SO ₄	Increase the extent of sodium salt dissolution by prolonged exposure of fibers to boiling water	~150 ppm (mass-based)
	Mobile Trapped H ₂ SO ₄	Non-neutralized or unwashed intra-fibrillar H ₂ SO ₄	Thorough washing in hot solvent aqueous bath	~70 ppm (mass-based)
Defect bands (planar defects)	NH ₃ ⁺ HSO ₄ ⁻ agglomerated chain ends	Coulombic forces induced clustering of ion-terminated chain ends	The phenomenon is not well understood so no remedy is obvious	One band every 40-60nm of fibril (ca. 3000ppm-mass-based))

* Extruded fibers



the case of yarns, weak inter-fiber) van der Waals / mechanical interlocking forces and to be less dependent on the fibril transverse mechanical properties.

The results obtained in this portion of the work can be summarized as follows:

(a) fibril stiffness was found to be affected by both the type and concentration of the defects. An example of the typical results pertaining to the effect of defect type/concentration on the PPTA-fibril stiffness is depicted in Figures 2(a)–(b). In Figure 2(a), the case of -COOH chain end defect was considered, while in Figure 2(b) the case of -SO₃H side group defect was analyzed;

(b) As far as the fibril axial strength was concerned, it was found to

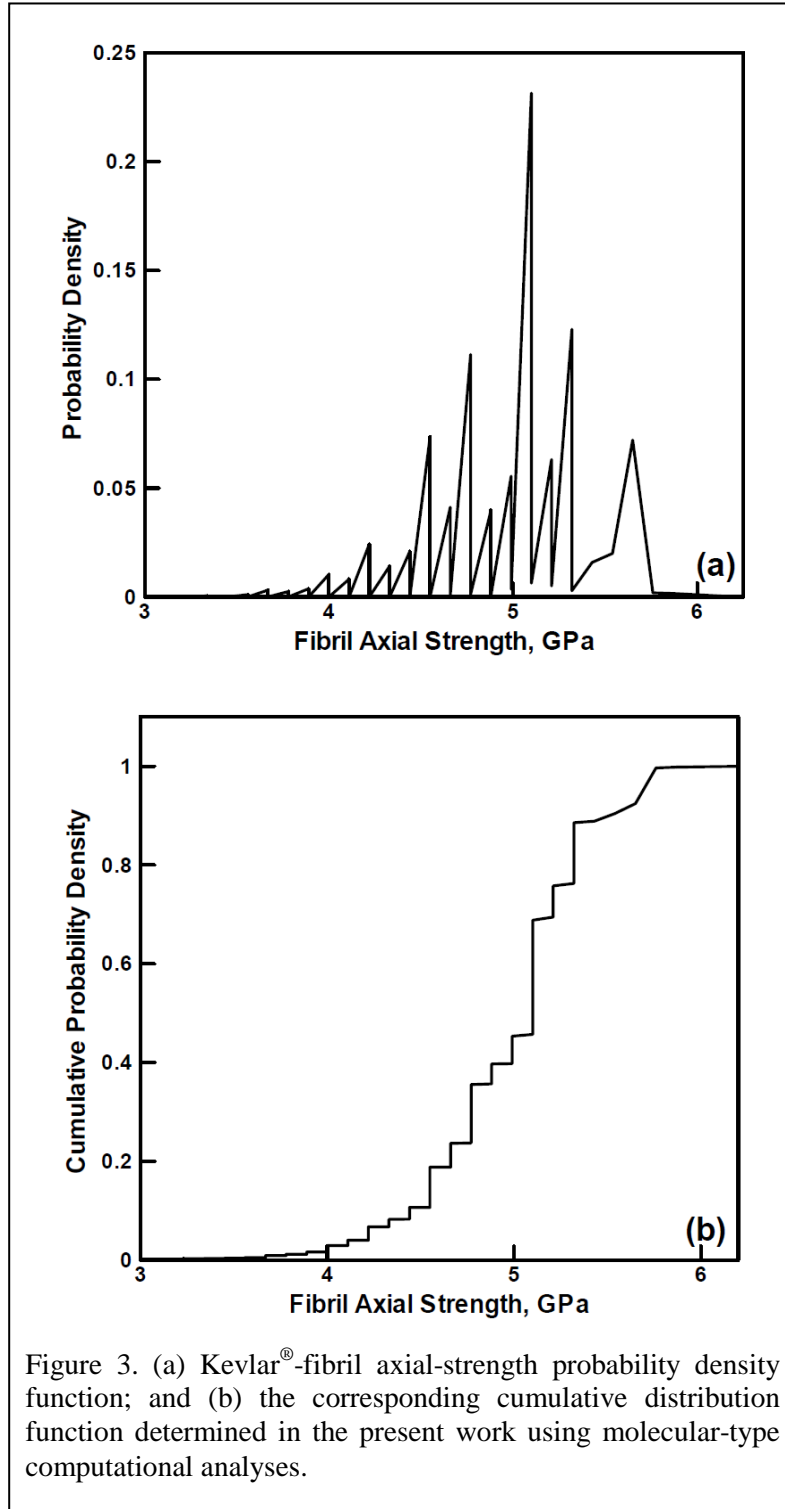
be affected by defect type and the size and composition of the largest defect cluster. Examples of typical results obtained are shown in Tables 2 and 3. The clusters composed of

Table 2. A summary of the effect of the most common defects found in Kevlar®-based materials and their (same defect-type) clusters on the PPTA fibril axial tensile strength (in GPa)

Flaw Group	Flaw	Number of defects in the largest cluster		
		1	2	3
Isolated chain ends (point defect)	-COOH	6.0	5.6	5.0
	-COO ⁻ Na ⁺			
	-NH ₂	6.1	5.8	5.2
	-NH ₃ ⁺ HSO ₄ ⁻			
Side Groups (point defect)	-SO ₃ H	5.8	5.1	4.1
	-SO ₃ ⁻ Na ⁺			
Voids and Interstitials (point defects)	Microvoids	3.8	N/A	N/A
	Mobile Trapped H ₂ SO ₄	3.9	N/A	N/A
Defect bands (planar defects)	NH ₃ ⁺ HSO ₄ ⁻ - agglomerated chain ends	3.2	N/A	N/A

Table 3. A summary of the effect of the composition and the size of the mixed SO₃H/SO₃⁻Na⁺ based side group and COOH/COO⁻Na⁺ based chain end defect clusters on the PPTA fibril axial tensile strength (in GPa)

		Number of SO ₃ H/SO ₃ ⁻ Na ⁺ defects in the cluster		
		1	2	3
Number of COOH/COO ⁻ Na ⁺ defects in the cluster	1	5.5	4.8	3.8
	2	5.3	4.4	3.4
	3	4.5	3.8	2.7



defects of the same type are considered in Table 2 while the effect of mixed-type defect (chain-end and side-group) clusters is considered in Table 3. Examination of the results reported in Tables 2 and 3 reveals that the extent of fibril axial-strength loss increases with the cluster size/strength;

(c) The aforementioned finding that the fibril axial strength is a function of the largest defect cluster and its composition indicated that fibril strength is a stochastic property. Hence, in the present work results like the ones displayed in Tables 2 and 3 are combined with the prototypical defect concentration densities, Table 1, in order to derive the associated PPTA fibril-strength distribution function, Figures 3(a)-(b);

(d) In accordance with the established topological

relationships between the fibrils, fibers and yarns, PPTA fibers are found to be transversely isotropic (with the fiber axis being the unique material direction) although the constituent fibrils possess orthotropic symmetry. Consequently, (i) fiber axial stiffness and strength, E_{11}

and σ_1 are found to be nearly equal to their fibril counterparts; (ii) the fiber transverse normal stiffness, $E_{22}=E_{33}$, is found to be nearly equal to the more compliant E_{33} fibril modulus; and (iii) All three shear moduli G_{12} , G_{13} and G_{23} are found to be nearly equal to the same value, the value which is controlled by the compliant PPTA inter-sheet sliding resistance (i.e. G_{12} of the fibrils); and

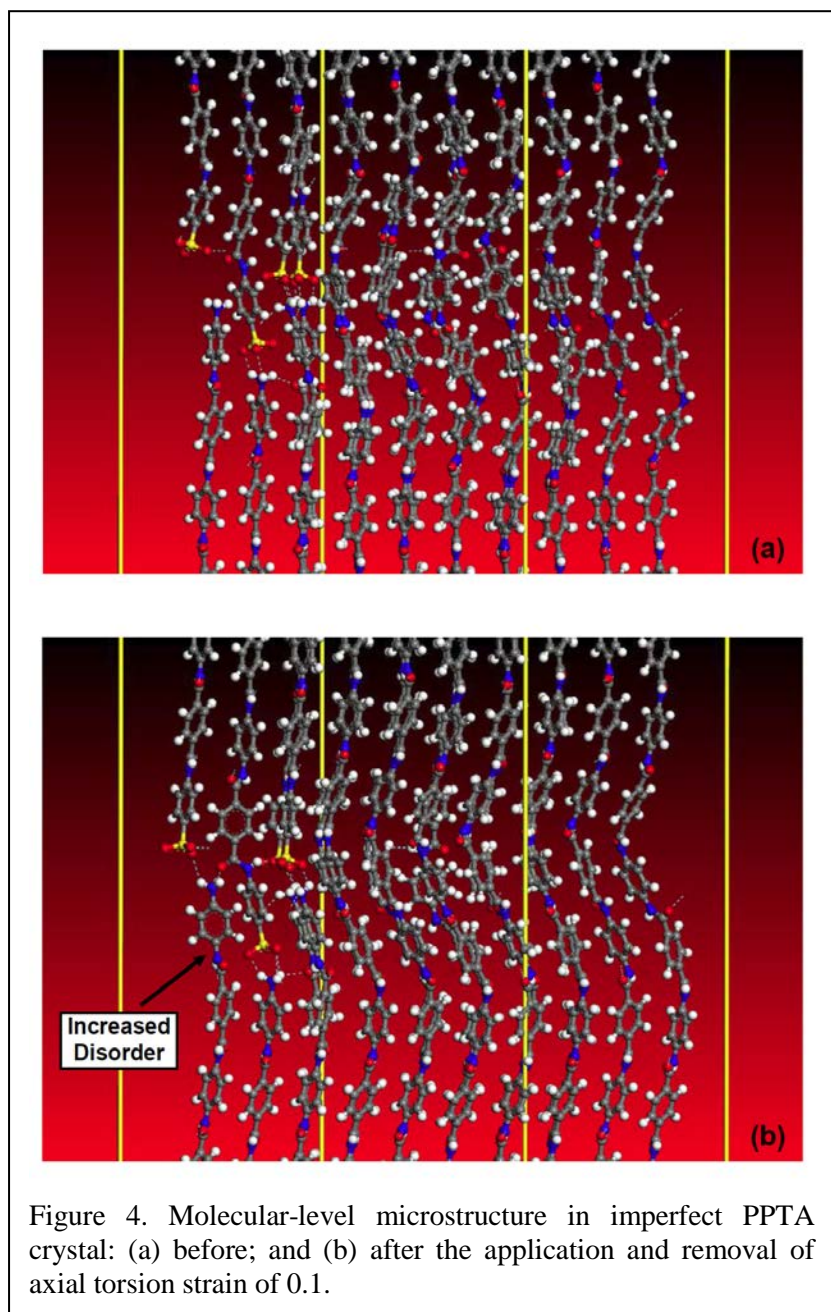
(e) To assess the yarn-level stiffness and strength properties from the known fiber properties, additional effects arising from the fiber-twist-induced inter-fiber friction had to be taken into account. This procedure mainly affected the yarn axial strength (or more precisely, yarn axial-strength distribution). It was generally found that the fibril-level axial strength distribution function displayed in Figures 3(a)-(b) was modified in the yarn case by an inter-fiber-friction dependent (positive) strength shift. For example, for a prototypical extent of fiber twist, an increase in the strength of ca. 0.2 GPa was found.

5.4 Effect of Fiber-/Yarn-Handling-Induced Defects on PPTA-Fiber Properties

During the weaving process used to produce the PPTA fabric, PPTA fibers/yarns (in particular, the warp fibers/yarns) can sustain substantial damage due to high bending and contact stresses. The resulting defects can also degrade mechanical properties of the PPTA-based materials, and their effect has to be accounted for in the analysis of the ballistic-protection resistance of the PPTA-based materials. To address this problem, a series of all-atom and coarse-grained molecular-level computational analyses is carried out in the present work [11–13]. Specifically, the effect of the preludial handling-induced deformation modes such as fiber/yarn transverse compression due to inter-yarn contacts, fiber/yarn twist/axial-compression, and fiber/yarn bending (encountered primarily in warp yarns) and the associated formation of kink-bands has been investigated. The results obtained revealed:

(a) high contact stresses can induce topological/crystallographic defects and, in turn, severely degrade the longitudinal-tensile strength of PPTA fibers/yarns, and significantly alter the associated PPTA-fiber longitudinal-strength probability distribution function;

(b) application of the prior axial torsion to the PPTA imperfect single-crystalline fibrils degrades their longitudinal-tensile strength and only slightly modifies the associated probability density function. This effect of the preludial axial torsion has been linked to the permanent changes in the fibril-/fiber-microstructure caused by this deformation mode. An



example of some changes is depicted in Figures 4(a)–(b). The results displayed in Figure 4(a) pertain to the microstructure before deformation, while Figure 4(b) shows the microstructure after the application and subsequent removal of the axial torsion associated with a maximum shear strain of 0.1. Examination of the results displayed in Figures 4(a)–(b) shows that the application of simple shear gives rise to some permanent changes in the PPTA microstructure. Specifically, under axial torsion, an increase in the extent of disorder is observed, particularly in the region adjacent to the single defect present in the

computational cell. This disorder is accompanied by a reduction in the number of hydrogen bonds. These residual changes in the PPTA-crystal microstructure are a probable reason that the prior axial torsion causes the changes in the PPTA-fiber longitudinal-tensile strength probability distribution function;

(c) The preludial axial compression can introduce (residual) kink bands into the PPTA fibers and, in turn, significantly degrade fiber longitudinal-tensile strength and its statistical

distribution. An example of the axial-compression-induced shear bands is depicted in Figure 5;

(d) fiber-fibrillation can also take place during axial compression, and give rise to the longitudinal-tensile strength and degradation, and changes in the strength probability density function. An example of the axial-compression-induced fiber-fibrillation is shown in Figure 6.

5.5 Development of a Continuum-Level Physically-Based Material Constitutive Model

PPTA-fiber-reinforced polymer matrix composite materials display quite complex deformation and failure behavior under ballistic/blast impact loading conditions. This complexity is generally attributed to a number of factors such as: (a) hierarchical/multi-length scale architecture of the material microstructure; (b) non-linear, rate-dependent and often pressure-sensitive mechanical response; and (c) the interplay of various intrinsic phenomena and processes such as fiber twisting, inter-fiber friction/sliding, etc. Material models generally employed in the computational engineering analyses of ballistic-/blast-impact protective structures made of this type of material do not typically include many of the aforementioned aspects of the material dynamic behavior. Consequently, discrepancies are often observed between computational predictions and their experimental counterparts. To address this problem, the results of an extensive set of molecular-level computational analyses carried out in the present work and overviewed earlier, regarding the role of various microstructural/morphological defects on the PPTA fibril/fiber/yarn mechanical properties, are used to upgrade one of the continuum-level material models for fiber-reinforced composites developed by Yen [14] of the Army Research Laboratory, Aberdeen Proving Ground, MD. The results obtained in the upgraded PPTA continuum-level material model [14–18] show that the response of the material is significantly affected as a result of the incorporation of microstructural effects both under quasi-static simple mechanical testing condition and under dynamic ballistic-impact conditions. This is demonstrated in Figure 7, in which typical results pertaining to the effect of projectile initial velocity on the projectile residual velocity in the case of the Yen [14] composite material model and its present modification are displayed. It is seen that V_{50} (defined here as the projectile initial velocity at which the projectile residual velocity is zero) predicted by the analysis in which the

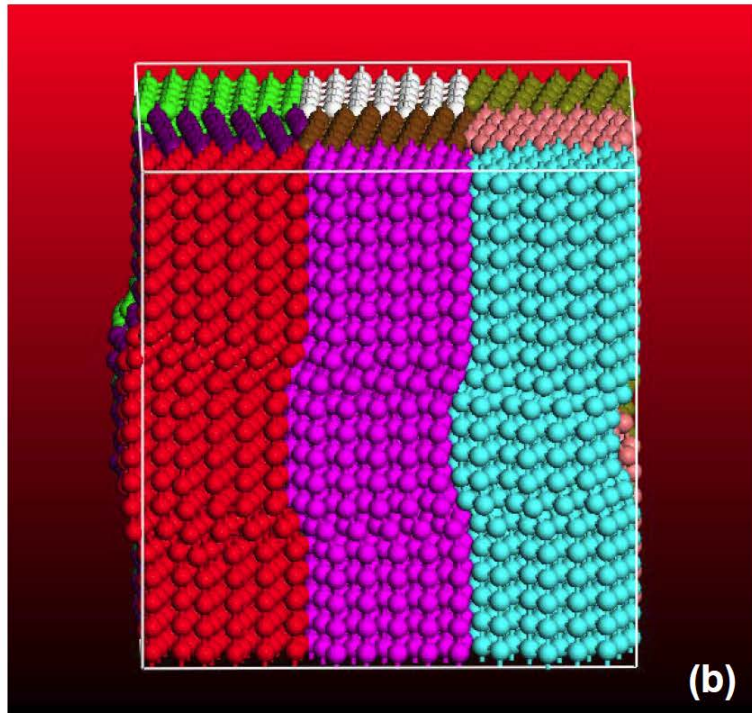
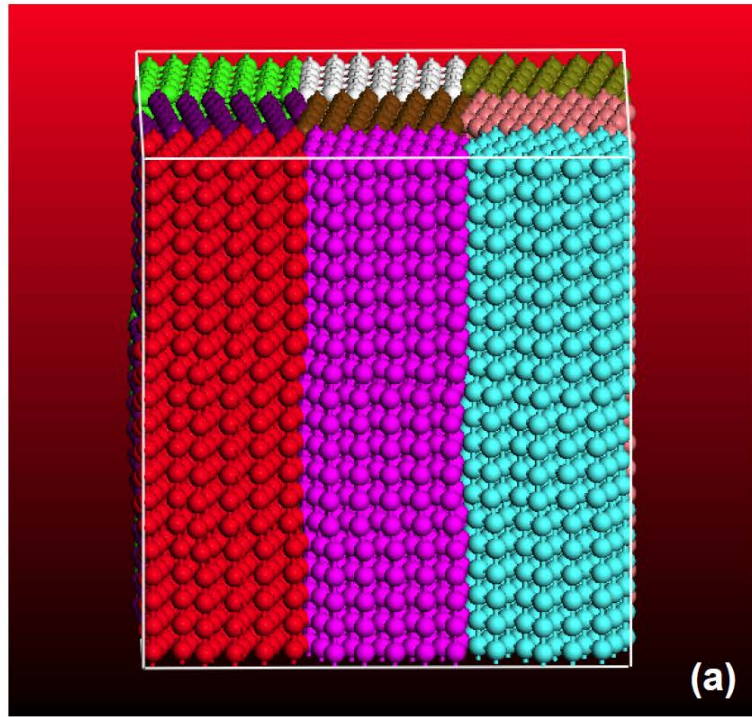


Figure 5. Coarse-grained microstructure, during axial compression, within the computational cell containing (initially) defect-free virgin PPTA fiber at the longitudinal stretch values of: (a) 0.975; (b) 0.950; (c) 0.925; and (d) 0.900.

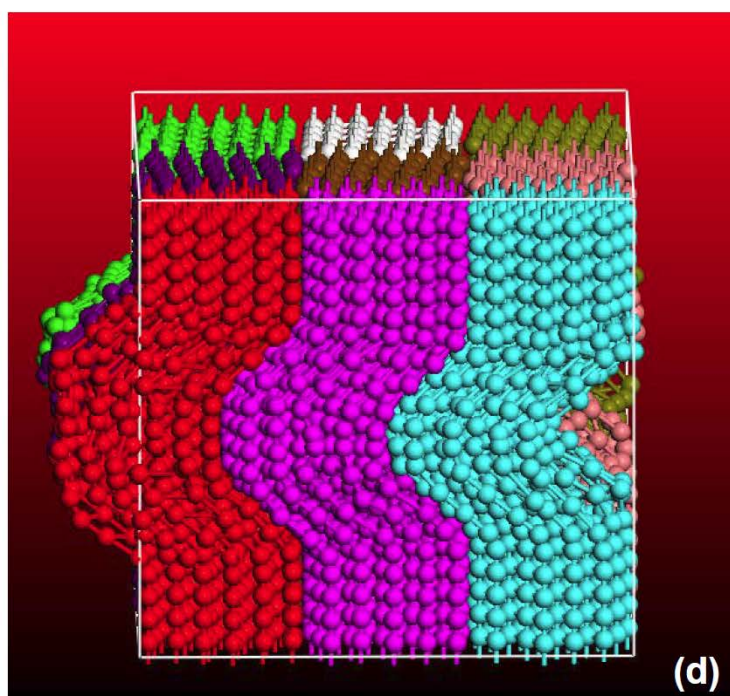
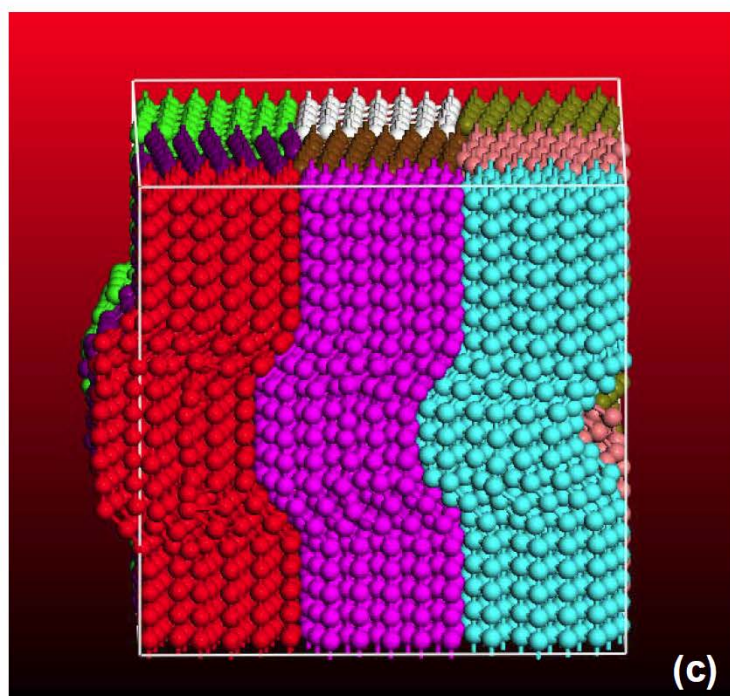


Figure 5. continued.

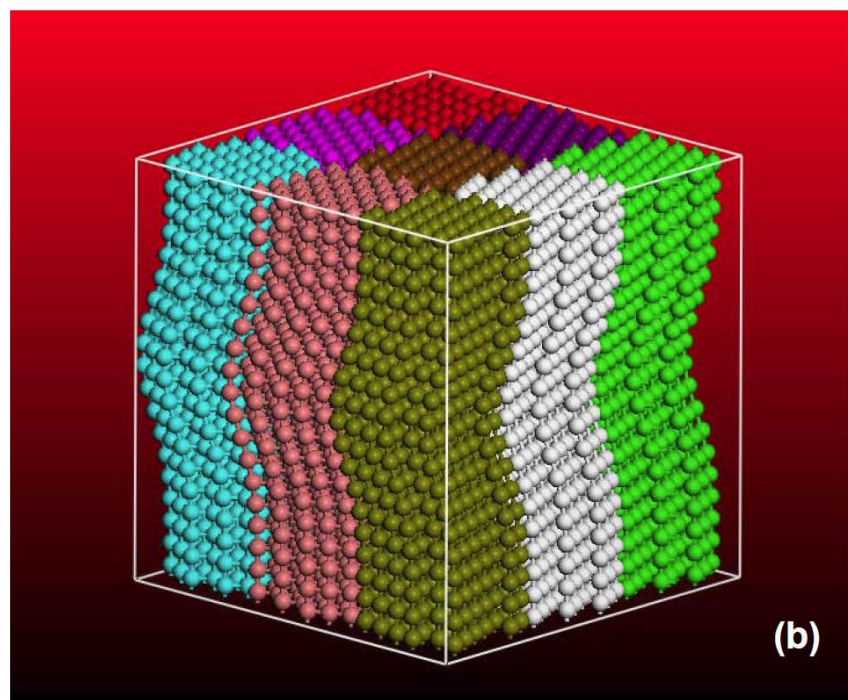
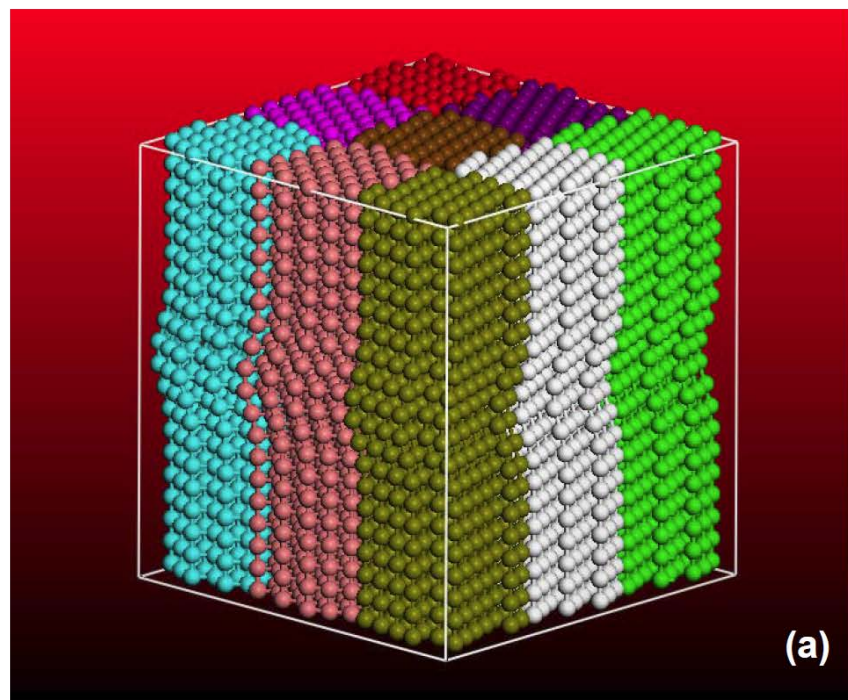


Figure 6. Coarse-grained microstructure, during axial compression, within the computational cell containing (initially) defective virgin PPTA fiber at the longitudinal stretch values of: (a) 0.975; (b) 0.950; (c) 0.925; and (d) 0.900. The fiber within the computational cell contains a cluster of side-group defects.

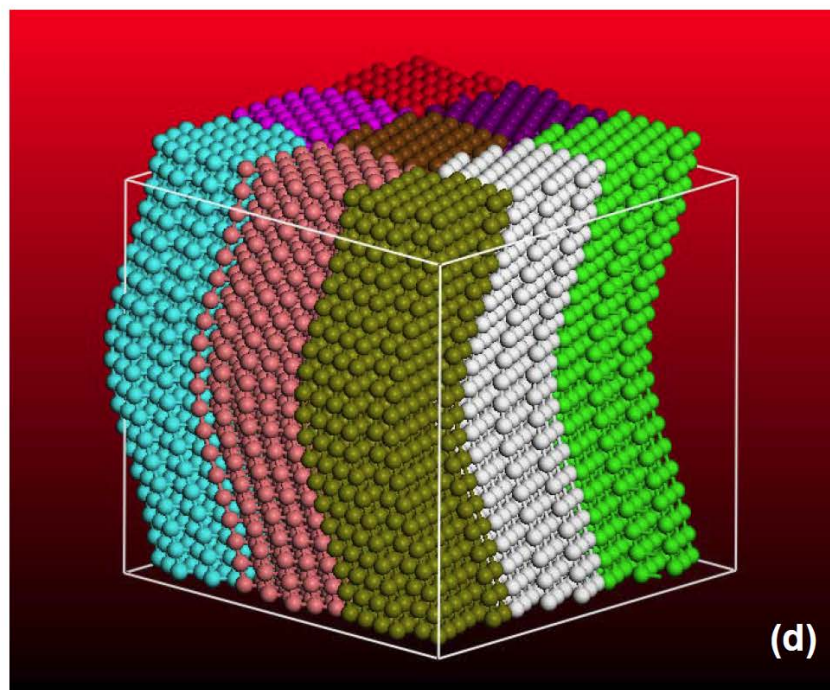
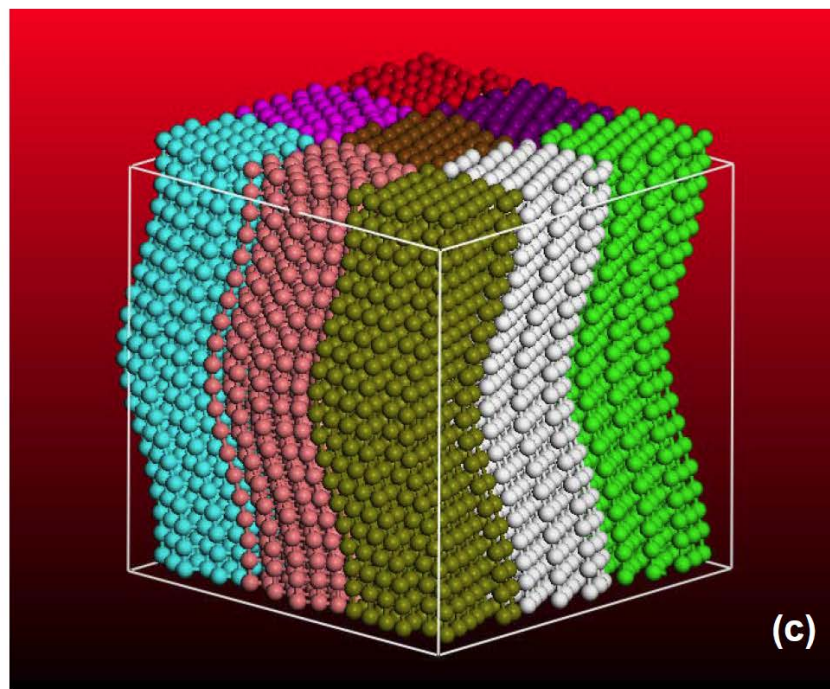


Figure 6. continued.

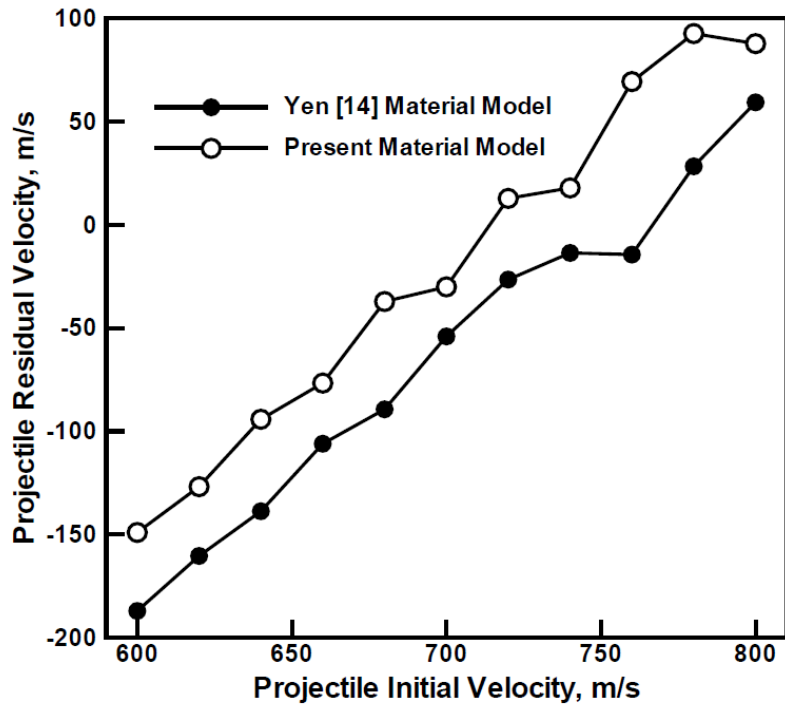
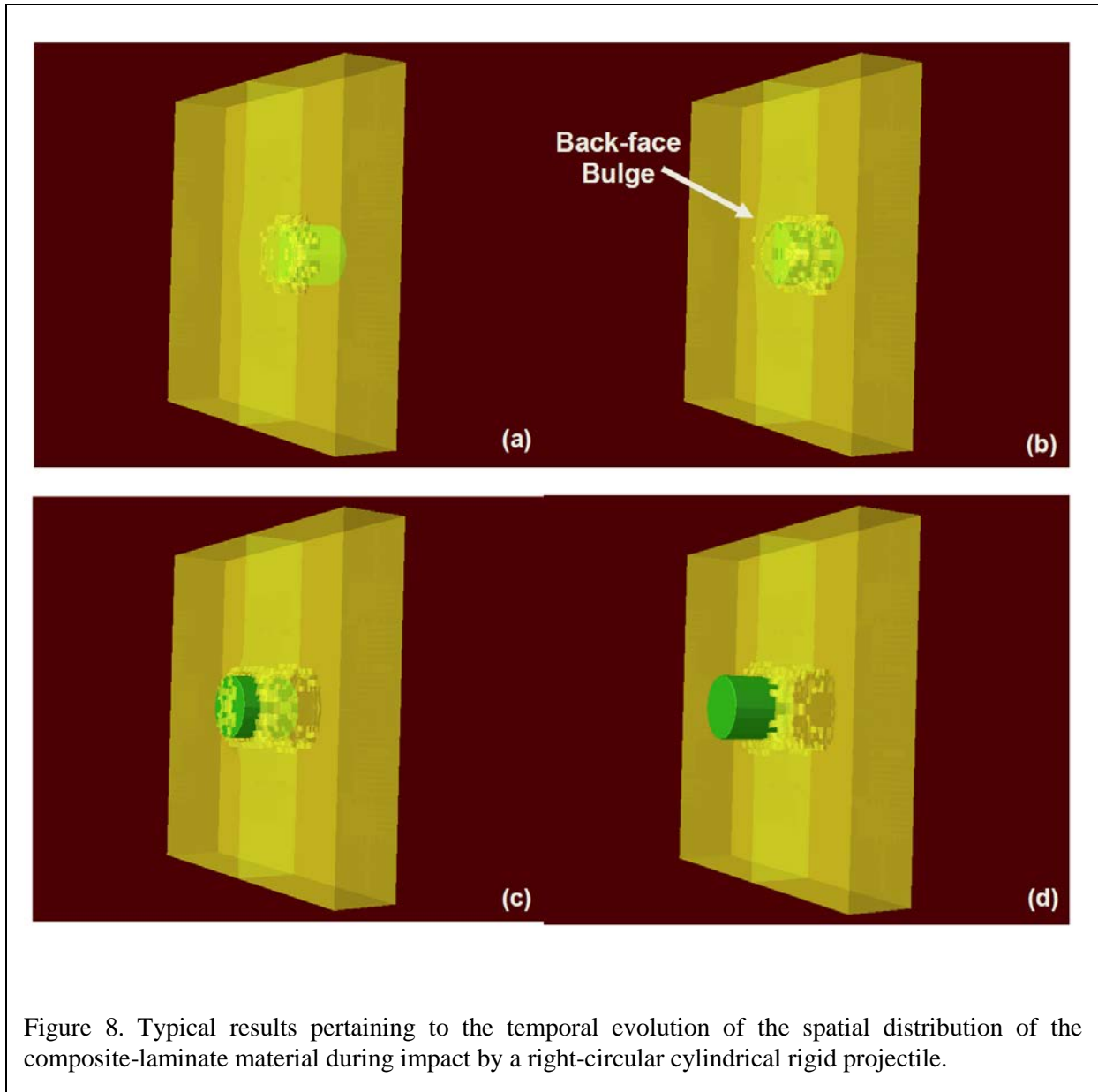


Figure 7. A typical projectile residual velocity vs. projectile incident velocity plot showing differences in V_{50} as predicted by the original Yen [14] material model and its upgrade proposed in the present work.

modified composite material model is used is ca. 5% lower than its counterpart associated with the use of the original Yen [14] composite material model. This effect is deemed as being significant and justifies the present efforts aimed at incorporating fine-scale microstructural effects into the continuum-level material model.

An example of the prototypical results obtained in the present work, pertaining to the ballistic-impact of a right-circular-cylindrical rigid projectile on a PPTA-fiber-reinforced composite laminate containing a poly-vinyl-ester-epoxy matrix, is given in Figures 8(a)-(d). The results displayed in Figures 8(a)-(d) pertain to the spatial distribution of the composite-laminate material during impact. It should be noted that in order to enable monitoring of the penetration process, the target plate is made transparent. The results displayed in Figures 8(a)-(d) clearly reveal the development of the back face bulge. In general, it was found that details regarding the spatial distribution and the temporal evolution of the target material during impact are significantly affected by the modifications made to the original Yen [14] composite material model.



6. Bibliography

1. M. Grujicic, W. C. Bell, P. S. Glomski, B. Pandurangan, C-F.Yen and B. A. Cheeseman, “*Filament-level Modeling of Aramid-based High-Performance Structural Materials*,” Journal of Materials Engineering and Performance, 20, 1401–1413, 2011.
2. M. Grujicic, W. C. Bell, P. S. Glomski, B. Pandurangan, C-F. Yen and B. A. Cheeseman, “*Multi-length Scale Computational Derivation of Kevlar® Yarn-level Material Model*,” Journal of Materials Science, 46, 4787–4802, 2011.
3. M. Grujicic, B. Pandurangan, K. L. Koudela and B. A. Cheeseman, “*A Computational Analysis of the Ballistic Performance of Light-Weight Hybrid-Composite Armor*,” Applied Surface Science, 253, 730–745, 2006.
4. M. Grujicic, T. He, H. Marvi, B. A. Cheeseman, C.-F. Yen, “*A Comparative Investigation of the Use of Laminate-level Meso-scale and Fracture-mechanics Enriched Meso-scale Composite-material Models in Ballistic Resistance Analyses*,” Journal of Materials Science, 45, 3136–3150, 2010.
5. M. Grujicic, D. C. Angstadt, Y.-P. Sun and K. L. Koudela, “*Micro-mechanics Based Derivation of the Materials Constitutive Relations for Carbon Nanotube Reinforced Poly-Vinyl-Ester-Epoxy Based Composites*,” Journal of Materials Science, 42, 2007, 4609-4623.
6. M. Grujicic, G. Arakere, T. He, M. Gogulapati and B. A. Cheeseman, “*A Numerical Investigation of the Influence of Yarn-Level Finite-Element Model on Energy Absorption by a Flexible-fabric Armor During Ballistic Impact*,” Journal of Materials: Design and Applications, 222, 2008, 259-276.
7. M. Grujicic, W. C. Bell, G. Arakere, T. He, X. Xie and B. A. Cheeseman, “*Development of a Meso-scale Material Model for Ballistic Fabric and its Use in Flexible-armor Protection Systems*,” Journal of Materials Engineering and Performance, 19-1, 2010, 22-39.
8. M. Grujicic, W. C. Bell, T. He and B. A. Cheeseman, “*Development and Verification of a Meso-scale based Dynamic Material Model for Plain-woven Single-ply Ballistic Fabric*,” Journal of Material Science, 43, 2008, 6301-6323.
9. B. A. Cheeseman, C. F. Yen, B.R. Scott, B. Powers, T.A. Bogetti, B. LaMatina, Y. Duan, M. Keefe, Y. Miao and Y. Wang, “*From Filaments to Fabric Packs – Simulating the Performance of Textile Protection Systems*,” ARL Report ADM002075, 2006.
10. S. M. Lee, *Handbook of Composite Reinforcements*, John Wiley and Sons, ISBN: 978-0-471-18861-2, 1993.
11. M. Grujicic, S. Ramaswami, J. S. Snipes, R. Yavari, G. C. Lickfield, C.-F. Yen and B. A. Cheeseman, “*Molecular-Level Computational Investigation of Mechanical Transverse Behavior of p-phenylene terephthalamide (PPTA) Fibers*,” Multidiscipline Modeling in Materials and Structures, 9, 462–498, 2013. DOI 10.1108/MMMS-11-2012-0018

12. M. Grujicic, R. Yavari, J. S. Snipes, S. Ramaswami, C.-F. Yen, and B. A. Cheeseman, “*Molecular-Level Study of the Effect of Prior Axial Compression/Torsion on the Axial-Tensile Strength of PPTA Fibers*,” Journal of Materials Engineering and Performance, 22, 3269–3287, 2013. DOI: 10.1007/s11665-013-0648-2
13. M. Grujicic, S. Ramaswami, J. S. Snipes, R. Yavari, C.-F. Yen and B. A. Cheeseman, “*Axial-Compressive Behavior, Including Kink-Band Formation and Propagation, of Single p-Phenylene Terephthalamide (PPTA) Fibers*,” Advances in Materials Science and Engineering, Volume 2013, Article ID 329549, 2013. DOI: 10.1155/2013/329549
14. C. F. Yen, “*A Ballistic Material Model for Continuous-Fiber Reinforced Composites*,” International Journal of Impact Engineering, 46, 11–22, 2012.
15. M. Grujicic, B. Pandurangan, J. S. Snipes, C.-F. Yen and B. A. Cheeseman, “*Multi-Length Scale Enriched Continuum-Level Material Model for Kevlar[®]-Fiber Reinforced Polymer-Matrix Composites*,” Journal of Materials Engineering and Performance, 22, 681-695, 2013. DOI: 10.1007/s11665-012-0329-6
16. M. Grujicic, A. Hariharan, B. Pandurangan, C.-F. Yen, B. A. Cheeseman, Y. Wang, Y. Miao and J. Q. Zheng, “*Fiber-level Modeling of Dynamic Strength of Kevlar[®] KM2 Ballistic Fabric*,” Journal of Materials Engineering and Performance, 21, 1107–1119, 2012. DOI: 10.1007/s11665-011-0006-1.
17. M. Grujicic, B. Pandurangan, W. C. Bell, C.-F. Yen and B. A. Cheeseman, “*Application of A Dynamic-mixture Shock-wave Model to the Metal-matrix Composite Materials*,” Materials Science and Engineering A, 528, 8187–8197, 2011.
18. M. Grujicic, W. C. Bell, B. Pandurangan, C.-F. Yen and B. A. Cheeseman, “*Computational Investigation of Structured Shocks in Al/SiC-particulates Metal Matrix Composites*,” Multidiscipline Modeling in Materials and Structures, 7, 469–497, 2011.